NASA TECHNICAL MEMORANDUM

NASA TM X-1822

NASA TM X-1822

NEUTRONIC COMPARISON OF BERYLLIUM OXIDE AND MOLYBDENUM FOR MOVABLE REFLECTOR CONTROL OF A FAST-SPECTRUM REACTOR

by Charles L. Whitmarsh, Jr., and Wendell Mayo

Lewis Research Center
Cleveland, Ohio

NATIONAL AERONAUTICS AND SPACE ADMINISTRATION • WASHINGTON, D. C. • JUNE 1969

NASA TM X-1822

NEUTRONIC COMPARISON OF BERYLLIUM OXIDE AND MOLYBDENUM FOR MOVABLE REFLECTOR CONTROL OF A FAST-SPECTRUM REACTOR

By Charles L. Whitmarsh, Jr., and Wendell Mayo

Lewis Research Center
Cleveland, Ohio

NATIONAL AERONAUTICS AND SPACE ADMINISTRATION

For sale by the Clearinghouse for Federal Scientific and Technical Information
Springfield, Virginia 22151 – CFSTI price $3.00

ABSTRACT

A neutronic comparison of beryllium oxide and molybdenum as the major constituents of axially translating radial reflectors for the reactivity control of a fast-spectrum reactor is made. Both one- and two-dimensional transport calculations are used. The analysis indicates that the multiplication factors, power distributions, and reactivity control worth are nearly the same for both types of reflector materials. The normally higher worth of the beryllium oxide reflector is reduced because of (1) the presence of molybdenum canning material in the reflector and a tantalum alloy pressure vessel between the core and the reflector and (2) the need to provide cooling and helium containment.

NEUTRONIC COMPARISON OF BERYLLIUM OXIDE AND MOLYBDENUM FOR MOVABLE REFLECTOR CONTROL OF A FAST-SPECTRUM REACTOR

by Charles L. Whitmarsh, Jr., and Wendell Mayo

Lewis Research Center

SUMMARY

A neutronic comparison of beryllium oxide (BeO) and molybdenum (Mo) as the major constituents of axially translating radial reflectors for the reactivity control of a fast-spectrum reactor is made. The reactor is fueled with enriched uranium-235 nitride in pin-type fuel elements utilizing molybdenum cladding and supported by a tantalum alloy (T-111) honeycomb. Three radial fuel zones with 31-, 35-, and 39-volume-percent fuel are used to make the power distribution more uniform. The coolant is lithium-7 (Li^7), and the 0.635-centimeter-thick pressure vessel with an outside diameter of 40 centimeters is T-111. The movable reflector, nominally 8.5 centimeters thick and located outside the pressure vessel, is split at the core midplane and slides toward the core ends. A 2.5-centimeter-thick stationary reflector forms the outermost extremity of the reactor. The volume percentages of the materials in the BeO reflector are 70 BeO, 10 Mo, and 10 Li^7. The Mo reflector is 95-volume-percent Mo.

Both of these reflectors were found to provide essentially the same excess reactivity, reactivity worth, and power distributions. The reactivity control swing was 10.79-percent $\Delta k/k$ for the BeO reflector and 11.11-percent $\Delta k/k$ for the Mo reflector. Perturbations to the reactor design external to the core were also found to have similar effects for both reflector materials. For example, small increases in pressure vessel diameter reduced the control swing by 1.0-percent $\Delta k/k$ per centimeter in both systems. However, the effect of increased pressure vessel thickness was greater for the BeO reflector; a reduction of 3.3-percent $\Delta k/k$ per centimeter, compared to 2.6-percent $\Delta k/k$ per centimeter for the Mo reflector, was calculated.

The effects due to various approximations in the calculations were examined. The number of energy groups, the angular quadrature order, and the geometrical symmetry assumptions were varied, and the results are reported.

INTRODUCTION

External control systems are particularly applicable to the compact, high-temperature nuclear reactors being considered in the space program (ref. 1). Control can be attained by movement of reflectors, which alters the fraction of neutrons returned to the reactor core. The method of reflector movement - rotation of drums and vanes or linear translation of slabs - used in a design depends on the specific application. Of interest in this report is a reflector control system which adjusts the leakage of neutrons by axial movement of a radial reflector surrounding a cylindrical reactor core.

On the basis of physical properties and low neutron absorption cross sections, beryllium oxide (BeO) and molybdenum (Mo) were selected as reflector materials. BeO is the lighter material but evolves helium as the result of neutron interactions, has relatively poor heat transfer, is not a good structural material, and is more susceptible to radiation damage (ref. 2). The importance of these factors in a design will depend on the specific application.

The purpose of this report is to provide a neutronics comparison between BeO and Mo when they are used as reflector materials. "Neutronics" is used herein as a general term indicating the behavior and effects resulting from neutron interactions with materials in nuclear reactors. This neutronics comparison is made from analytical determinations of reactivity worths and power distributions. Reactivity worth of a reflector represents the maximum amount of reactivity that can be controlled by operating the reflector between its position extremes - full in to full out. Additional calculations are made to indicate reactivity effects of design changes external to the reactor core, such as pressure vessel thickness and diameter, on both BeO and Mo reflected reactors.

Reflector characteristics are inherently sensitive to reactor size, flux spectrum, and reflector configuration. The study presented herein is concerned with the control of a compact, fast-spectrum, liquid-metal-cooled reactor which could operate at 1.8 megawatts thermal for 50 000 hours with a coolant outlet temperature of 1140 K (1600° F). To meet these operating conditions, the reflector control system must be worth 7.7-percent reactivity to include allowances for fuel burnup, core expansion, Doppler effect, manufacturing tolerances, reactor shutdown, and a one-stuck-element safety criterion.

REACTOR MODEL

From heat-transfer and criticality analyses, a reactor model was developed which consists of a T-111 cylindrical pressure vessel packed with uranium nitride ($U^{235}N$) fuel pins and surrounded by a reflector. The fuel pins are clad with molybdenum and are

positioned in a T-111 honeycomb structure which also provides flow passages for the lithium-7 (Li^7) coolant (fig. 1).

A major source of stress in the fuel cladding is the buildup of fission gas pressure during reactor operation. In order to reduce these stresses three radial zones were established, with the concentration of $U^{235}N$ in a fuel pin being varied between zones. The fuel loading arrangement is shown in figure 2, where equivalent diameters for use in one-dimensional or two-dimensional R-Z calculations are indicated by dashed lines. These cylindricized zones were converted from the actual geometry by conserving the total atoms of each material in each zone.

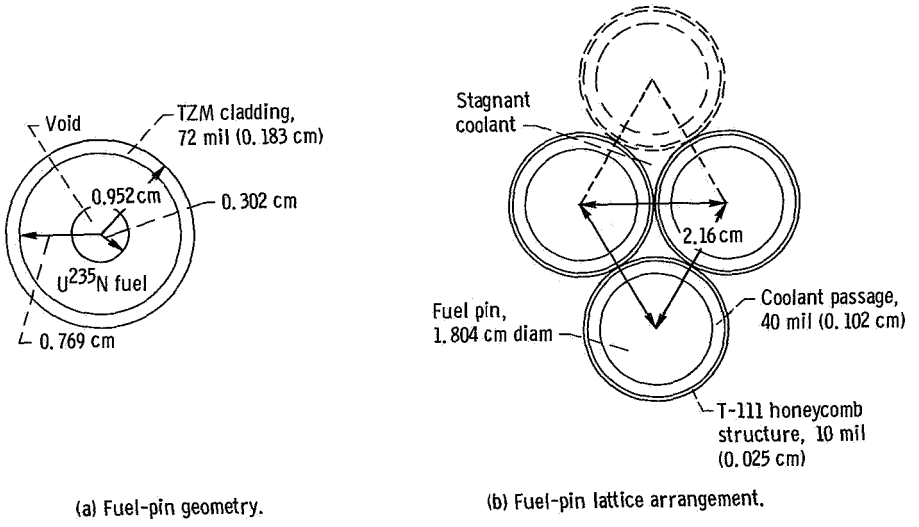

(a) Fuel-pin geometry.

(b) Fuel-pin lattice arrangement.

Figure 1. - Reactor fuel pins.

The radial reflector consisted of cylindrical shells, with the inner 8.5-centimeter-thick section being movable and the outer 2.5-centimeter-thick section being stationary. The stationary reflector was constructed from Mo with Li^7 cooling passages occupying 15 percent of the volume. The movable reflector required no internal cooling when Mo was used as the construction material, but a 5-percent void was allowed for clearances. When BeO was considered for the movable reflector, 10 percent of the volume was allocated for a self-contained Li^7 cooling system, 10 percent for Mo canning material, and a 10-percent void to contain helium (He) production. It is assumed that lithium does not fill the space vacated when the reflector moves out. These allowances were estimated requirements based on the lower thermal conductivity of BeO, its susceptibility to radiation damage, and its He-producing interaction with neutrons.

At each end of the core is a mixing chamber composed of 90-percent Li^7 and 10-percent T-111 and a stationary reflector of 85-percent Mo and 15-percent Li^7.

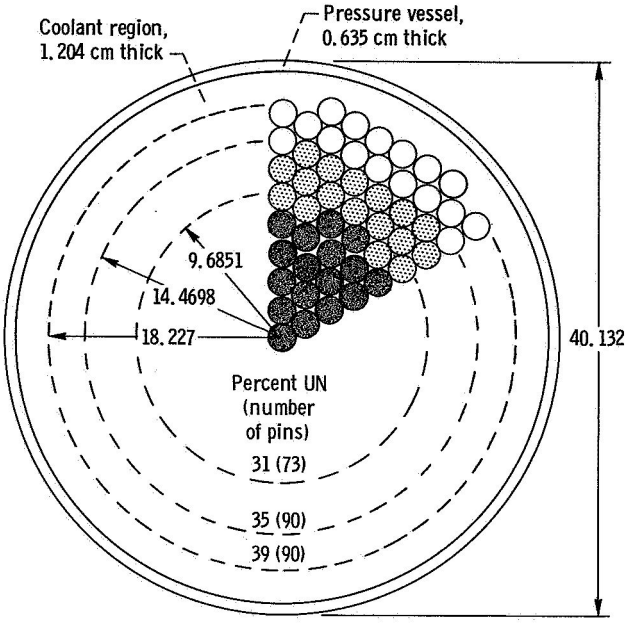

Figure 2. - Fuel zoning geometry. Dimensions are in centimeters.

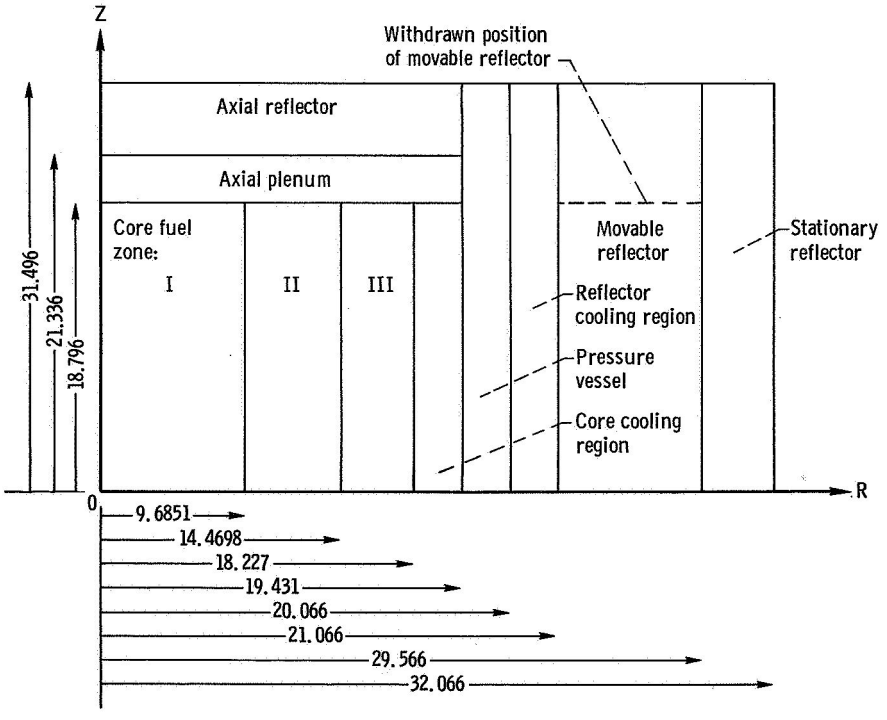

Figure 3. - Reactor calculational model. Dimensions are in centimeters.

TABLE I. - MATERIALS FOR REACTOR MODEL

Material	Density, g/cm^3	Core fuel zone			Core cooling region	Axial plenum	Pressure vessel	Reflector cooling region	Movable reflector		Stationary reflector
		I	II	III					BeO	Mo	
		Volume, percent									
$U^{235}N$	14.2	31	35	39	---	--	---	--	--	--	--
Li^7	.51	25.2	25.2	25.2	100	90	---	90	10	--	15
Mo	10.2	24.5	24.5	24.5	---	--	---	--	10	95	85
[a]T-111	16.72	4.2	4.2	4.2	---	10	100	10	--	--	--
BeO	3.025	----	----	----	---	--	---	--	70	--	--
Void	------	15.1	11.1	7.1	---	--	---	--	10	5	--

[a]Weight percentages of constituents of T-111 used in calculations are 2.3 hafnium, 8.5 tungsten, and 89.2 tantalum.

Cooling regions exist along the inside and the outside of the pressure vessel. The calculational model shown in figure 3 was derived from the physical model and indicates the regions of importance and their dimensions. Material compositions of the various regions are listed in table I.

Shielding around the reactor was not considered in this analysis, although it might be present in a real situation. However, shield effect was estimated from data on similar reactor configurations where a - 1-percent $\Delta k/k$ change in control swing was calculated for an 8-centimeter-thick layer of lithium-6 hydride placed adjacent to the stationary reflector.

It is estimated that operation at 1.8-megawatt-thermal power for 50 000 hours will require about 7.7-percent $\Delta k/k$ for reactivity control. Of this total, 1.5-percent $\Delta k/k$ is for fuel burnup, 1.0-percent $\Delta k/k$ is for temperature-induced expansion of the Li^7 and the core, 0.2-percent $\Delta k/k$ for total Doppler effect, 1.0-percent $\Delta k/k$ for manufacturing and fuel loading tolerances, 2-percent $\Delta k/k$ for normal shutdown margin, and 2.0-percent additional $\Delta k/k$ to allow shutdown when one control element is stuck. Therefore, reflector control swing (reactivity that can be regulated by reflector movement) must be $\geq$7.7-percent $\Delta k/k$ and the actual multiplication factor k of the fully reflected, cold, clean reactor must be $\sim$1.04.

CALCULATIONAL PROCEDURE

All criticality calculations were performed with the neutron transport computer program TDSN (ref. 3) using neutron cross sections generated by the programs GAM-II (ref. 4) for energy groups above 0.414 electron volt and GATHER-II (ref. 5) for energy groups below 0.414 electron volt. These cross sections were averaged over a fast spectrum similar to the actual core spectrum (see appendix A). Another set of cross sections, averaged over a moderating material spectrum, was used for the radial reflector regions when BeO was considered as the movable reflector material.

Several code options are available in the use of TDSN depending on the desired degree of calculational sophistication (and presumably accuracy). To illustrate the notation scheme used to designate these code options, a one-dimensional S_4P_0 14-group problem would (1) approximate the actual geometry in one dimension, (2) use the fourth-order angular quadrature scheme for solving the S_n transport equations, (3) use cross sections determined from the first term P_0 Legendre polynomial expansion solution to the transport equation and which contain a correction to approximate nonisotropic scattering, and (4) use a cross-section set based on 14 discrete energy groups.

Theoretically, the accuracy of a solution from a TDSN calculation is dependent on the use of these code options - the higher the order of each option, the greater the accu-

racy. Ideally then, all problems would be run with the highest possible code options. However, because of such difficulties as extended machine running time, complexity of problem setup, and limited machine storage capacity, it is desirable to do most of the calculations with lower-order options. For example, we would like to be able to predict accurate high-order solutions by using a low-order calculational result plus a correction.

Corrections to the multiplication constant were determined by comparison of calculations performed with various combinations of code options. These data are presented in table II. Generally, throughout the study reported herein, parametric analyses were made with one-dimensional S_4P_0 14-group calculations, with a reflector savings of 13.5 centimeters to simulate axial leakage. Whenever desired, these results could be corrected to two-dimensional S_4P_0 14-group accuracy by the use of table II. Although

TABLE II. - EFFECT OF CALCULATION DETAIL ON MULTIPLICATION FACTOR

Change in calculation	70-Volume-percent BeO movable reflector		95-Volume-percent Mo movable reflector	
	Reflector inserted, $^a k = 1.1025$	Reflector withdrawn, $^a k = 0.9853$	Reflector inserted, $^a k = 1.1065$	Reflector withdrawn, $^a k = 0.9854$
	Change in multiplication factor, k			
Energy groups:				
5 to 14	-0.0089	-0.0051	-0.0004	-0.0014
SN order:				
2 to 4	-.0116	-.0147	-.0123	-.0148
Geometry:				
one- to two-dimensional	.0050	-.0072	.0088	-.0061

[a]Assumed best value which has been corrected to a two-dimensional S_4P_0 14-group calculation.

the highest order calculation actually performed was a two-dimensional S_4P_0 5-group calculation, a two-dimensional S_4P_0 14-group result could be synthesized, and this was considered to be the "best" result.

The use of data from table II can be extended to other reactors as long as problem similarity is maintained (i.e., the geometry and the materials of the reactor must be similar to the BeO and Mo reflected fast-spectrum reactor configurations in this study).

Reflector worth was determined from two calculations of the multiplication factor, one with the movable reflector fully in and one with the movable reflector withdrawn to the ends of the core (fig. 3). The change in reactivity caused by reflector movement was then calculated from

$$\text{Reflector worth in units of percent } \Delta k/k = \frac{k_1 - k_2}{k_1 k_2} \times 100$$

where

k_1 multiplication factor with reflector inserted

k_2 multiplication factor with reflector withdrawn

ANALYSIS AND RESULTS

This section consists of three major parts. The first part is a discussion of multiplication factors k and reflector control worth. The second part is concerned with spatial power distributions. The third part consists of reactivity effects and coefficients resulting from perturbations in reactor regions external to the core. However, the effects due to movable reflector thickness and material composition appear in the first two parts.

Reactivity and Reflector Worth

Multiplication factors for the BeO and Mo reflected and unreflected reactor configurations are listed in table II. These values represent the "best" multiplication factors calculated in this study (two-dimensional S_4P_0 14-group calculation). An 8.5-centimeter-thick movable reflector is used for all cases in the table. The reflector is withdrawn only to the length of the active core, as indicated in figure 3.

A large variation in the correction factor for changing energy groups from 5 to 14 groups was observed for the BeO reflected configuration compared to the Mo reflected configuration. However, the correction factors for S_n order and geometry were similar for the two systems. This indicates the greater sensitivity to the detail used in defining energy spectra for calculations containing BeO.

As indicated in figure 3, the geometry for a one-dimensional calculation is the same for either the BeO or Mo reflector-withdrawn cases. Thus, one-dimensional multiplication factors derived from columns 2 and 4 of table II should have the same value. Small differences were noted, however, which were probably due to the different spectra over which the cross sections were averaged. In the two-dimensional reflector-withdrawn cases, reflectors were withdrawn only to the ends of the core (fig. 3), thereby leaving a portion of the reflector in the calculational geometry.

The worths of the movable reflectors are given in table III. The estimated worth using correction factors from table II for the two-dimensional S_4P_0 14-group calculation is 10.79-percent $\Delta k/k$ with the BeO reflector and 11.11-percent $\Delta k/k$ with the Mo reflector. Reference 6 indicates that BeO is a substantially better reflector than Mo.

TABLE III. - REFLECTOR WORTH COMPUTED BY VARIOUS MODELS

Calculation			70-Volume-percent BeO	95-Volume-percent Mo
Geometry, dimensions	Quadrature order	Energy groups	Reflector worth, percent Δk/k	
2	S_2	5	10.44	10.50
1	S_4	14	9.64	9.76
2	S_4	14	[a]10.79	[a]11.11

[a]Estimated values using correction factors from table II.

In the present case, however, the density of BeO in the reflector has been reduced to 70-volume-percent BeO, and 10-volume-percent Mo has been added as a canning material. The Mo is a moderately effective neutron absorber in the resonance and thermal neutron energy range. In addition, a further negation of the moderating effect of the BeO is due to the presence of the T-111 pressure vessel (see appendix B). The result is a reflector that is very nearly equivalent to the Mo reflector.

Again, referring to table III, it is observed that the lower-order two-dimensional calculations (two-dimensional S_2P_0 5-group) are to be preferred over the one-dimensional high-order calculations (one-dimensional S_4P_0 14-group) in predicting control worth. Compared to the "best" value (two-dimensional S_4P_0 14-group calculations) obtained by applying inferred correction factors (from table II), the use of one-dimensional calculations results in discrepancies in control worth of -1.15-percent Δk/k for the 70-volume-percent BeO reflected reactor and -1.35-percent Δk/k for the 95-volume-percent Mo reflected reactor. The low-order two-dimensional calculations underpredict the control worth by about 0.3- and 0.6-percent Δk/k, respectively, for the BeO and Mo reflected reactors.

The one-dimensional model was used to determine reflector worth for various thicknesses of the movable reflector, as shown in figure 4. The control worth obtained is about the same for BeO and Mo reflectors over the range of reflector thicknesses from 4.5 to 8.5 centimeters; for example, the 70-volume-percent BeO reflector worth varied from 7.3- to 9.6-percent Δk/k, and the 95-volume-percent Mo reflector worth varied from 7.1- to 9.7-percent Δk/k, respectively. In these calculations, as the movable reflector thickness was decreased, the stationary reflector was moved toward smaller radii but its thickness of 2.5 centimeters was maintained.

Multiplication factors as a function of movable reflector thickness are given in fig-

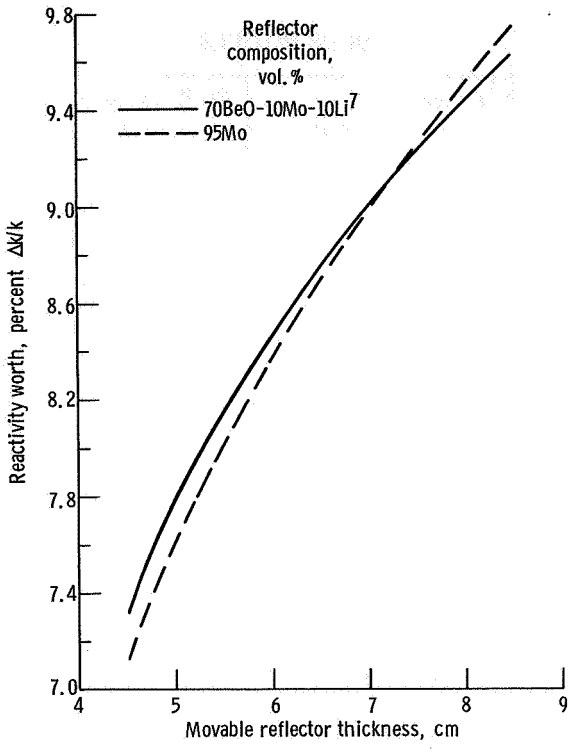

Figure 4. - Effect of reflector thickness on reactivity worth of movable radial reflectors based on one-dimensional S_4P_0 14-group calculations.

ures 5(a) and (b). Figure 5(a) shows the multiplication factors of the reflected reactor configuration, and figure 5(b) shows those of the reactors with movable reflectors withdrawn. Not only do the control worths for the two reflector materials agree, as shown in figure 4, but so do the multiplication factors shown in figures 5(a) and (b).

As noted previously, the small difference in k for the reflector-withdrawn curves of figure 5 is due to microscopic cross sections averaged over different spectra and not due to material differences, since the geometry for the one-dimensional calculations is the same for both cases.

The BeO reflectors are subject to radiation damage. For these systems, neutron fluence is about 10^{22} neutrons per square centimeter, which exceeds by a factor of 10 the value at which powdering of BeO occurs (ref. 2). Hence, BeO is canned in Mo of sufficient amount to withstand released helium pressure in the reflector (thereby accounting for the 10-percent Mo in the BeO reflector). Since the actual amount required is uncertain, the effect of increasing the Mo content in the BeO reflector was investigated. Figure 6 shows how the control swing and k vary as a function of the percentage of BeO in the reflector. The auxiliary scale of figure 6 shows the corresponding amount of Mo; the 10-percent void and 10-percent Li^7 remain constant. The control swing changed by less

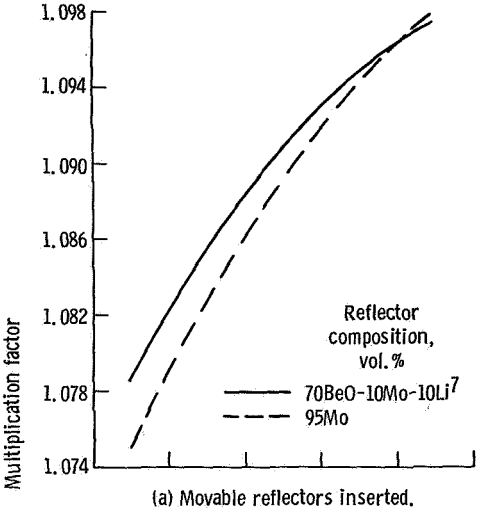

Figure 5. - Effect of movable reflector thickness on multiplication factor based on one-dimensional S_4P_0 14-group calculations.

than 0.5-percent $\Delta k/k$ and the multiplication constant by 0.6-percent $\Delta k/k$ for a reduction in BeO of from 70 to 30 percent. This small penalty indicates that control and excess reactivity are not sensitive to the composition of the BeO-Mo reflector. Figure 6 also shows that on an equal volume percent basis BeO is worth slightly more than Mo as a reflector for this reactor; that is, changing 40 volume percent of the reflector from BeO to Mo decreases the reflector worth by 0.48-percent $\Delta k/k$. It should be noted, however, that the previous comparison of reflectors (table III) was not made on this basis.

Power Distributions

A comparison of radial power distributions indicated little difference between BeO and Mo reflected reactors (fig. 7). These data were obtained with two-dimensional S_2P_0 5-group TDSN calculations of reactor configurations with 8.5-centimeter movable

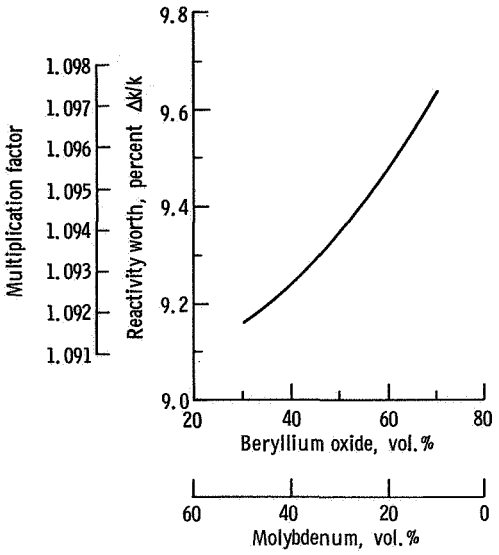

Figure 6. - Effect of varying beryllium oxide and molybdenum content of movable reflector on reactivity worth and multiplication factor of reflected reactor configuration based on one-dimensional S_4P_0 14-group calculations. Multiplication factor for unreflected reactor, 0.9925.

reflectors inserted. Local-to-average power ratios $P/\overline{p}$ tended to peak at the inner edge of each fuel zone, and the maximum $P/\overline{p}$ in the core (1.41 for Mo and 1.39 for BeO reflectors) occurred at the core center. The fact that power peaking near the core edge (sometimes observed in BeO reflected reactors (ref. 6)) did not occur can be attributed to the absorption of low-energy neutrons by the T-111 pressure vessel between the core and the reflector (see discussion appendix B).

Variation of radial power shape with the extremes of reflector position is indicated by comparing figures 8(a) and (b). As the movable reflector is withdrawn, $P/\overline{p}$ tends to increase in the central fuel zone (1.39 to 1.68 at the center of a BeO reflected reactor) and decrease in the peripheral zone. Such behavior is characteristic since the reflector returns neutrons to the core which would otherwise leak out. These neutrons are absorbed primarily in the peripheral fuel region, thereby increasing the power generation there. Since the central fuel zone is essentially unaffected by these reflected neutrons, this increased power generation in the peripheral zone causes the relative power to decrease in the central zone.

As before, the effect on power distribution calculations of using various code options was determined by comparison of one-dimensional S_4P_0 5-group and 14-group and two-dimensional S_2P_0 5-group and S_4P_0 5-group results. The S_2 and S_4 comparisons

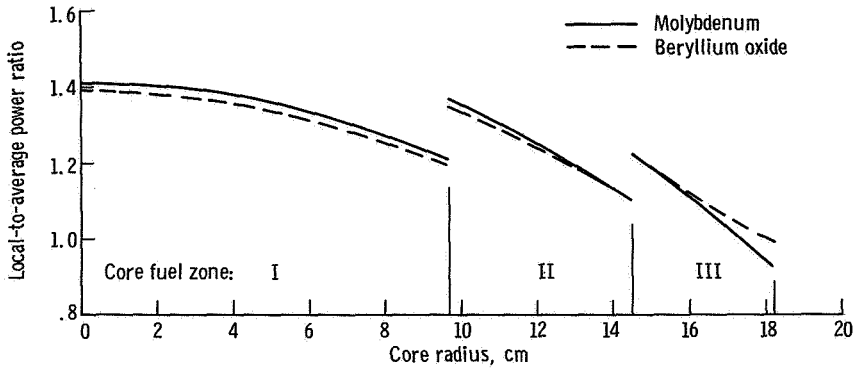

Figure 7. - Power distributions along radial plane at axial center of core with beryllium oxide and molybdenum reflectors, based on two-dimensional S_2P_0 5-group calculations.

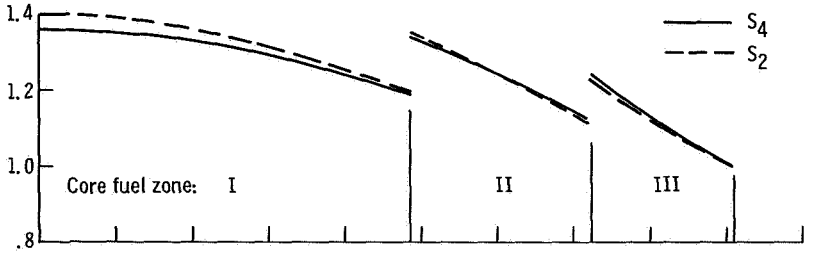

(a) Movable reflector inserted.

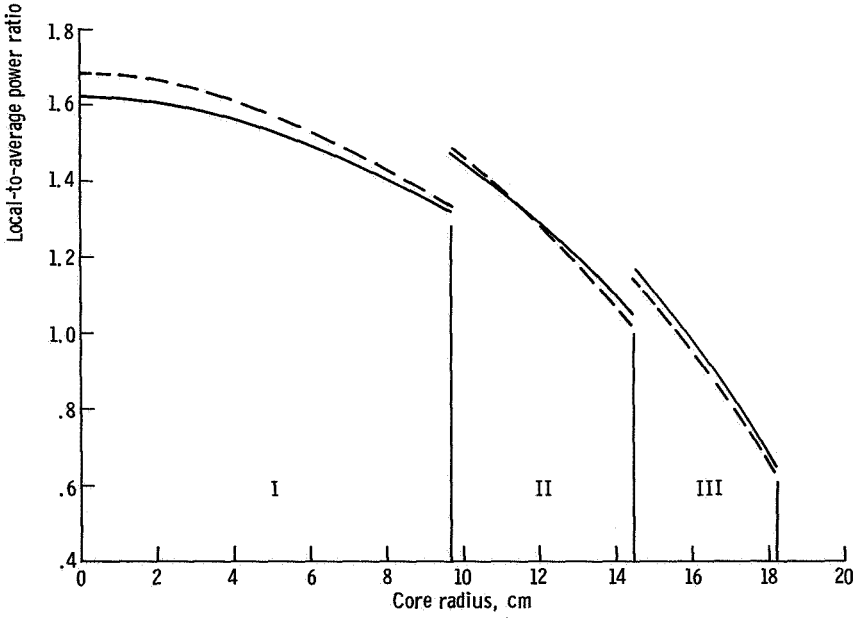

(b) Movable reflector withdrawn.

Figure 8. - Power distributions for beryllium oxide reflector control method showing effect of S_2 against S_4 two-dimensional 5-group calculations at axial center of core.

for a BeO reflected reactor with the movable reflector inserted and withdrawn (figs. 8(a) and (b), respectively) show less than a 4-percent variation of $P/\overline{p}$ in the core. The S_4 power ratios were lower in the central fuel zone and higher in the peripheral zone. The energy group comparison showed less than a 1-percent variation in $P/\overline{p}$ calculated with 5 energy groups and with 14 energy groups. At any point in a radial plane at the axial center of the core, the ratio of power densities from two-dimensional and one-dimensional calculations was constant (a factor of 1.19), thereby indicating the adequacy of using one-dimensional calculations to predict power shapes (fig. 9).

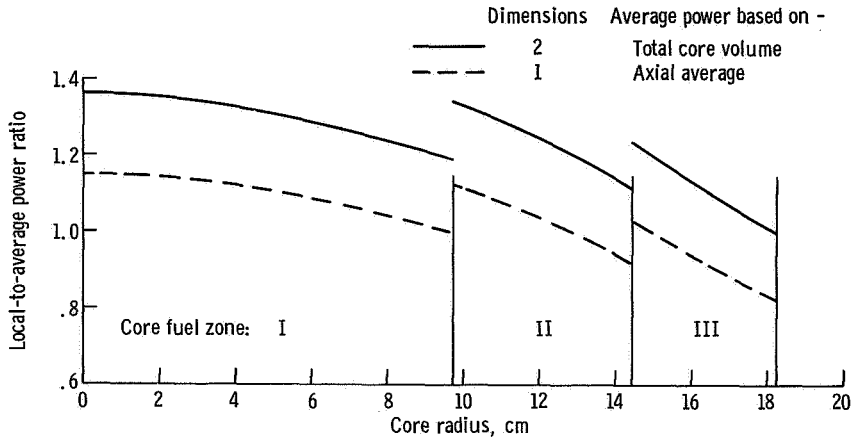

Figure 9. - Comparison of two-dimensional and one-dimensional S_4 5-group calculated power distributions for beryllium oxide reflected reactor configuration.

These correction factors were used to change the power peaking factors stated previously in this section (table IV). Thus, the peak value of $P/\overline{p}$ in the reactor core is 1.36 for the 70-volume-percent BeO reflected configuration and 1.37 for the 95-volume-percent Mo reflected configuration. For the unreflected configuration, the peak $P/\overline{p}$ is 1.63. All of the peak values of $P/\overline{p}$ occurred at the core center.

In general, as the moderating effect of a reflector decreases, the power ratio tends to increase in the central core region and decrease near the core edge. Such effects were noted when Mo was substituted for BeO and when BeO reflector thickness was reduced. However, changes in $P/\overline{p}$ were relatively small, for example, a maximum variation of 3 percent in $P/\overline{p}$ when reflector composition (in vol.%) was varied from 70BeO-10Mo-10Li^7 to 30BeO-50Mo-10Li^7 and a maximum variation of 2 percent when the BeO movable reflector thickness was reduced from 8.5 to 4.5 centimeters. A summary of the peak-to-average power ratios for each fuel zone is presented in table IV, where all results have been corrected to two-dimensional S_4P_0 14-group calculations.

TABLE IV. - PEAK-TO-AVERAGE POWER RATIOS FOR COMPACT (R = 18.227 CM) ZONED-CORE, REFLECTOR-CONTROLLED, HIGH-TEMPERATURE, LIQUID-METAL-COOLED NUCLEAR REACTOR WITH SEVERAL REFLECTOR CONFIGURATIONS

Reflector configuration			Core fuel zone		
Pressure vessel thickness, cm	Reflector composition, vol. %	Reflector	I	II	III
[a]8.5	70BeO-10Mo-10Li^7	Inserted	1.36	1.34	1.24
[a]8.5	70BeO-10Mo-10Li^7	Withdrawn	1.63	1.48	1.17
[a]8.5	95Mo	Inserted	1.37	1.36	1.24
[b]8.5	30BeO-50Mo-10Li^7	Inserted	1.39	1.36	1.24
[b]4.5	70BeO-10Mo-10Li^7	Inserted	1.41	1.36	1.23
[b]4.5	70BeO-10Mo-10Li^7	Withdrawn	1.60	1.45	1.18

[a]Values from two-dimensional S_2 5-group calculations which have been corrected to two-dimensional S_4 14-group calculation.

[b]Since only one-dimensional radial power shapes were calculated, results were synthesized from axial power shapes obtained from two-dimensional calculations on similar systems. The factor for converting one-dimensional radial power densities to two-dimensional radial power densities at the axial center of the core is 1.19.

Design Perturbations

Reactivity coefficients for various pressure vessel diameters and wall thicknesses were calculated to indicate the consequences of possible reactor design changes. Such changes could result from higher temperature reactor designs requiring thicker pressure vessels, and from the pressure vessel diameter being a function of the required amount of structural support for the core. Also, the effect of removing the reflector cooling region (which might be possible if a high-emissivity coating material on the reflector surfaces could provide sufficient cooling) was determined. These values are itemized in table V for both 70-volume-percent BeO and 95-volume-percent Mo reflected reactors. Reflector worth was reduced about 1.0-percent $\Delta k/k$ per centimeter increase of pressure vessel diameter and about 3.3-percent $\Delta k/k$ per centimeter increase in pressure vessel wall thickness for the BeO reflected reactor. Comparable values for the Mo reflected reactor were 1.0- and 2.6-percent $\Delta k/k$, respectively. Reducing the pressure vessel diameter tended to reduce the multiplication factor of the fully reflected reactor but had very little effect in the movable-reflector-withdrawn configuration.

TABLE V. - CRITICALITY EFFECTS OF DESIGN PERTURBATIONS[a]

Design parameter	70-Volume-percent BeO movable reflector			95-Volume-percent Mo movable reflector		
	Reactivity worth, percent Δk/k per centimeter[b]	Reflected	Unreflected	Reactivity worth, percent Δk/k per centimeter[b]	Reflected	Unreflected
		Reactor multiplication factor, percent k per centimeter[b]			Reactor multiplication factor, percent k per centimeter[b]	
Increasing pressure vessel internal diameter	-1.0	-1.27	-0.07	-1.0	-1.27	-0.07
Increasing pressure vessel thickness	-3.3	-1.46	2.03	-2.6	-.68	2.00
Removal of 1-centimeter-thick reflector cooling region	1.47	1.25	-.43	1.34	1.10	-.44

[a]Numerical values represent only one combination of parametric conditions. Additional calculations for all combinations yielded a data variation spread of less than ±30 percent.

[b]Per centimeter change of design parameter.

Increasing pressure vessel thickness also decreased the multiplication factor of the fully reflected reactor but had a larger and opposite effect (increased k) in the movable-reflector-withdrawn configuration. The primary effect of increasing the pressure vessel diameter is movement of the reflector farther from the core. Increasing pressure vessel thickness also has this effect, but of more importance is the reflectivity effect of the additional pressure vessel material, which shows up as increased k for the reflector-withdrawn configuration.

Removal of the 1-centimeter-thick reflector cooling region causes an increase of about 1.5-percent $\Delta k/k$ in reflector worth for the BeO reflected reactor and 1.3-percent $\Delta k/k$ for the Mo reflected reactor. The major effect here is movement of the reflector closer to the core, which increases the k of the reflected reactor. A lesser effect is the removal of moderating (and somewhat reflecting) material, which tends to decrease the k of the reactor with the movable reflector withdrawn.

SUMMARY OF RESULTS

The following results apply to a movable-reflector-controlled fast-spectrum nuclear reactor consisting of a 36.4-centimeter-diameter core fueled with $U^{235}N$ and cooled with Li^7. A 2.5-centimeter-thick Mo shell surrounds the radial reflector. The core is separated into three radial zones with the UN concentration varying from 31 volume percent in the central zone to 39 volume percent in the peripheral zone.

The overall result of this study was that, from the standpoint of excess reactivity, reactivity worth, and power shapes, no significant difference exists between a 70BeO-10Mo-10Li^7-volume-percent reflector and a 95-volume-percent Mo reflector. Detailed results are itemized as follows:

1. The reactivity worth of an 8.5-centimeter-thick 70BeO-10Mo-10Li^7-10 void radial reflector was 10.79-percent $\Delta k/k$. This value represents the best estimate from the results of one-dimensional and two-dimensional calculations. For an 8.5-centimeter-thick 95Mo-5 void radial reflector, the reactivity worth was 11.11-percent $\Delta k/k$.

2. The use of one-dimensional calculations underpredicted the worth of the 8.5-centimeter 70-volume-percent BeO reflector by 1.15-percent $\Delta k/k$ and that of the 8.5-centimeter 95-volume-percent Mo reflector by 1.35-percent $\Delta k/k$.

3. Reactivity worth of the 8.5-centimeter-thick reflector was insensitive to replacement of BeO with Mo (e.g., changing 40 volume percent of the reflector from BeO to Mo decreased the reflector worth 0.48-percent $\Delta k/k$).

4. Based on one-dimensional calculations, the worth varied from 7.3- to 9.6-percent $\Delta k/k$ for a thickness range of 4.5 to 8.5 centimeters with a BeO reflector and from 7.1- to 9.7-percent $\Delta k/k$ with a 95-volume-percent Mo reflector for the same thickness range.

5. With an 8.5-centimeter-thick 70-volume-percent BeO reflector, the peak-to-average power ratio in the core was 1.36 with the reflector fully inserted and 1.62 with the reflector withdrawn. In both configurations, the power peak occurred at the core center.

6. Peak-to-average power ratio was increased from 1.36 to 1.41 by a reduction in reflector thickness from 8.5 to 4.5 centimeters and increased from 1.36 to 1.39 by substituting Mo instead of BeO in the 8.5-centimeter-thick case.

7. Radial power distributions were relatively insensitive to changes in calculational method. Variations in peak-to-average power ratios were less than 4 percent between S_2 and S_4 calculations, and less than 1 percent between 5-group and 14-group calculations. Also two-dimensional power shapes along the core midplane were adequately predicted by one-dimensional calculations.

8. For a 70-volume-percent BeO reflected reactor, small increases in pressure vessel diameter and in thickness were calculated to reduce control swing by 1.0- and 3.3-percent $\Delta k/k$ per centimeter, respectively. Comparable values for the Mo reflected reactor were 1.0- and 2.6-percent $\Delta k/k$ per centimeter. Removal of the reflector cooling region from the reference reactor increased the control swing by 1.5-percent $\Delta k/k$ for the BeO reflected reactor and by 1.3-percent $\Delta k/k$ for the Mo reflected reactor.

Lewis Research Center,
National Aeronautics and Space Administration,
Cleveland, Ohio, March 17, 1969,
120-27-06-18-22.

APPENDIX A

ADDITIONAL CONSIDERATIONS IN CHOICE OF CALCULATIONAL MODEL

For criticality calculations of all reactor configurations which did not contain BeO, the thermal group of the 14-group and 5-group cross-section sets was dropped (table VI). Without BeO no effective thermal neutron moderating material was present in the reactor, and therefore most neutrons either leaked out or were absorbed before their energy could be degraded to the thermal level. So few neutrons were moderated to low energies that it could be assumed that no loss in the accuracy of reactivity and power distribution values resulted from the use of these 13-group and 4-group cross-section sets. The incentive for elimination of the thermal energy group was the considerable savings in computer time which resulted from the elimination of a relatively difficult convergence in an energy level with few neutrons.

Both the 14-group and 5-group cross-section sets were based on the infinitely dilute material approximation (i.e., resonances were not treated explicitly in the GAM calculation). This approximation tends to overestimate cross sections in the resonance energy regions, and as a result fluxes in a corresponding criticality calculation are undervalued. In order to check the significance of this effect in the present study, a 25-group set of cross sections was generated (for use in BeO moderated configurations) which had group energy spans adjusted to better define the resonance energies (table VI). For example, compared to the 14-group set, the lower energy groups were much finer and the span of the higher energy groups was widened. Cross sections for the core materials were flux weighted over a core spectrum using the homogeneous resonance approximation in GAM-II, and the cross sections for the remaining materials were weighted over a reflector spectrum with the slab resonance approximation being used for the T-111 pressure vessel. For configurations without BeO, all cross sections were weighted over a core spectrum using the homogeneous resonance approximation.

A comparison of data from criticality calculations performed with both the 14-group and 25-group cross-section sets is presented in table VII. A small discrepancy of less than 1-percent Δk occurred in the multiplication factor of the reflected configurations. The lower values, which were calculated with the 25-group set, can be attributed to the shifting of high-energy groups because analysis of the code output indicates that all the discrepancy occurs above 5.5 kiloelectron volts. The multiplication factor of the unreflected configuration and selected power ratio data indicated no significant effect on those values.

TABLE VI. - ENERGY GROUP SPLIT FOR

CROSS-SECTION SETS

Lower energy boundary, eV	Cross-section set		
	25-Group	14-Group	5-Group
[a]3.68×10^6	1	1	
2.23×10^6	2	2	1
1.35×10^6		3	
$.821\times10^6$		4	
$.498\times10^6$	3	5	2
$.302\times10^6$		6	
$.183\times10^6$		7	
$.111\times10^6$		8	3
40.9×10^3	4	9	
15.0×10^3	5	10	
5.53×10^3		11	
3.35×10^3	6	12	
2.03×10^3	7		
1.23×10^3	8		
$.749\times10^3$	9		
$.454\times10^3$	10		4
$.275\times10^3$	11		
$.167\times10^3$	12		
$.101\times10^3$	13		
61.4	14		
37.3	15		
22.6	16		
1.37	17	13	
8.32	18		
5.04	19		
3.06	20		
1.86	21		
1.13	22		
.683	23		
.414	24		
0	25	[b]14	[b]5

[a]Upper energy boundary of group 1 is 14.9 MeV.

[b]This group was dropped to form the 13- and 4-group sets.

TABLE VII. - COMPARISON OF CRITICALITY CALCULATIONS WITH 14-GROUP, INFINITELY DILUTE AND 25-GROUP, RESONANCE CORRECTED CROSS-SECTION SETS

Cross-section set	Movable reflector		Multiplication factor	Local-to-average power ratio[a]		
	Composition, vol. %	Position		I	II	III
14-Group	70BeO-10Mo-10Li^7	Inserted	1.0975	1.15	1.11	1.01
25-Group	70BeO-10Mo-10Li^7	↓	1.0890	1.17	1.11	↓
[b]13-Group	95Mo	↓	1.0977	1.17	1.12	↓
25-Group	95Mo	↓	1.0909	1.19	1.13	↓
[b]13-Group	----------	Withdrawn	.9925	1.36	1.20	.95
25-Group	----------	Withdrawn	.9934	1.36	1.20	.95

[a]At mesh point nearest inner edge of each fuel zone.

[b]Same as 14-group set except thermal group has been dropped.

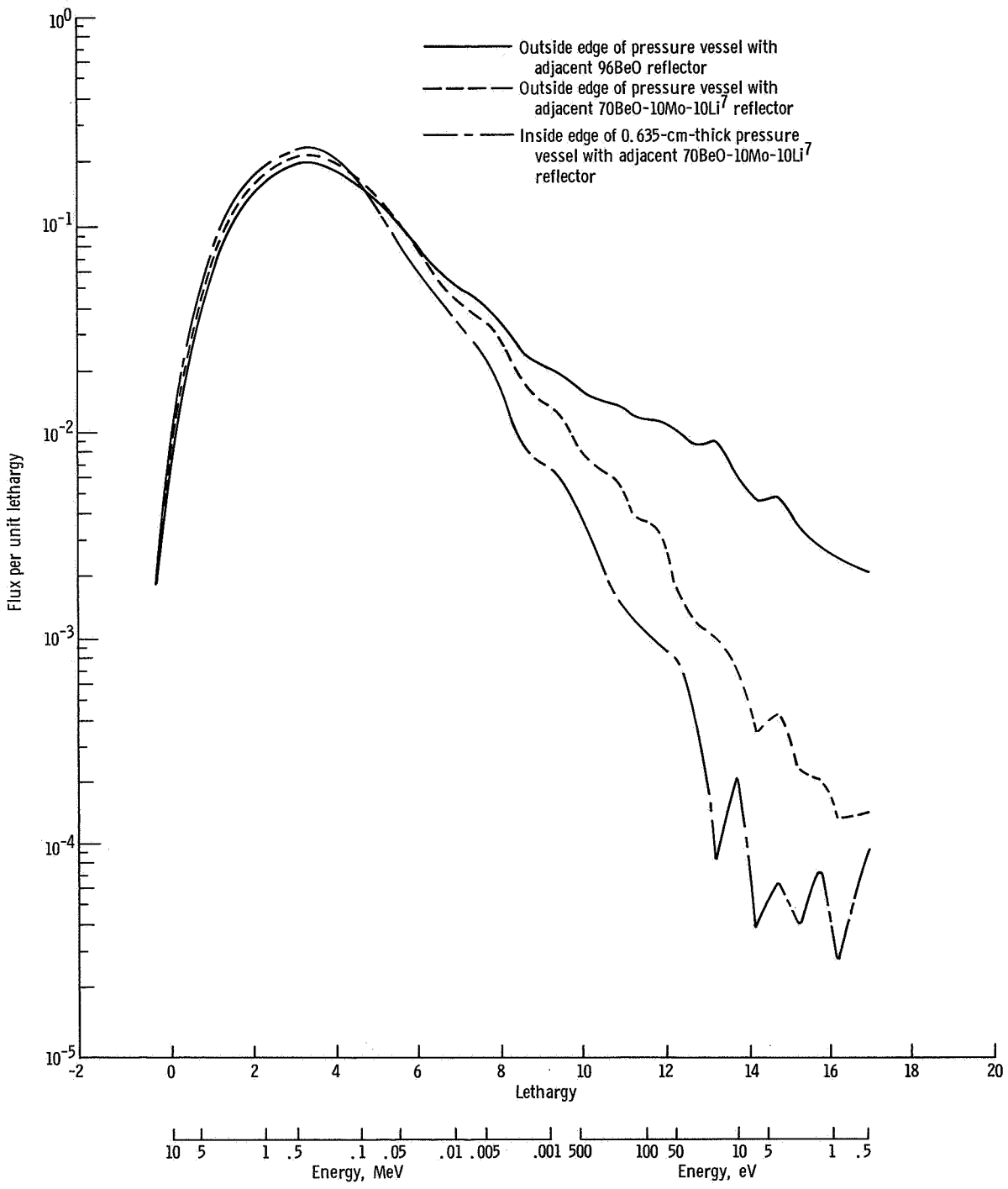

Figure 10. - Flux spectra near pressure vessel in reflected fast reactor configurations.

APPENDIX B

REFLECTED NEUTRON SPECTRAL EFFECTS

One of the differences noted between heavy and light materials, when they are used as reflectors for fast-spectrum reactor cores, is the energy spectrum of the reflected neutrons. The lower energy spectrum resulting from the use of a light-material reflector, such as BeO, tends to enhance the core reactivity effect of the reflected neutrons. However, in realistic designs, the inclusion of structural materials in and around the reflectors tends to alter the flux spectrum of the reflected neutrons prior to reentry into the core. Since the structural materials of interest will generally be refractory heavy metals, this alteration is a spectrum hardening (i.e., depletion of low-energy neutrons, which thereby increases the average neutron energy) when the reflector is composed of a relatively light material. This, in turn, tends to nullify the extra reactivity worth of a light-material reflector compared to a heavy-material reflector from the standpoint of spectral effects.

To illustrate this, spectra from a fast reactor configuration (fig. 3 and table I) have been plotted in figure 10. The difference between the solid and dashed lines represents the spectral hardening caused by the inclusion of 10-percent Mo in a reflector containing only BeO. These spectra existed at the outer edge of the pressure vessel. Additional hardening indicated by the dashed and broken curves results when the returning neutrons pass through a 0.635-centimeter-thick T-111 pressure vessel.

REFERENCES

1. Mason, D. G.; and Johnson, R. A.: Snap 8 Reactor Status Review. Paper 68-1116, AIAA, Oct. 1968.

2. Keilholtz, G. W.; Lee J. E., Jr.; and Moore, R. E.: Irradiation Damage to Sintered Beryllium Oxide as a Function of Fast-Neutron Dose and Flux at 110, 650, and 1100° C. Nucl. Sci. Eng., vol. 26, no. 3, Nov. 1966, pp. 329-338.

3. Barber, Clayton E.: A Fortran IV Two-Dimensional Discrete Angular Segmentation Transport Program. NASA TN D-3573, 1966.

4. Joanou, G. D.; and Dudek, J. S.: GAM-II. A B_3 Code for the Calculation of Fast-Neutron Spectra and Associated Mutligroup Constants. Rep. GA-4265, General Atomic Div., General Dynamics Corp., Sept. 16, 1963.

5. Joanou, G. D.; Smith, C. V.; and Vieweg, H. A.: GATHER-II, An IBM-7090 FORTRAN-II Program for the Computation of Thermal-Neutron Spectra and Associated Multigroup Cross Sections. Rep. GA-4132, General Dynamics/Fort Worth, July 8, 1963.

6. Lantz, Edward; Mayo, Wendell; Westfall, Robert M.; and Anderson, John R., Jr.: Small High-Temperature Nuclear Reactors for Space Power. NASA TN D-4371, 1968.

NASA-Langley, 1969 —— 22 E-4900

NATIONAL AERONAUTICS AND SPACE ADMINISTRATION
WASHINGTON, D.C. 20546

OFFICIAL BUSINESS

FIRST CLASS MAIL

POSTAGE AND FEES PAID
NATIONAL AERONAUTICS AND
SPACE ADMINISTRATION

POSTMASTER: If Undeliverable (Section 158
Postal Manual) Do Not Return

"The aeronautical and space activities of the United States shall be conducted so as to contribute . . . to the expansion of human knowledge of phenomena in the atmosphere and space. The Administration shall provide for the widest practicable and appropriate dissemination of information concerning its activities and the results thereof."

—NATIONAL AERONAUTICS AND SPACE ACT OF 1958

NASA SCIENTIFIC AND TECHNICAL PUBLICATIONS

TECHNICAL REPORTS: Scientific and technical information considered important, complete, and a lasting contribution to existing knowledge.

TECHNICAL NOTES: Information less broad in scope but nevertheless of importance as a contribution to existing knowledge.

TECHNICAL MEMORANDUMS: Information receiving limited distribution because of preliminary data, security classification, or other reasons.

CONTRACTOR REPORTS: Scientific and technical information generated under a NASA contract or grant and considered an important contribution to existing knowledge.

TECHNICAL TRANSLATIONS: Information published in a foreign language considered to merit NASA distribution in English.

SPECIAL PUBLICATIONS: Information derived from or of value to NASA activities. Publications include conference proceedings, monographs, data compilations, handbooks, sourcebooks, and special bibliographies.

TECHNOLOGY UTILIZATION PUBLICATIONS: Information on technology used by NASA that may be of particular interest in commercial and other non-aerospace applications. Publications include Tech Briefs, Technology Utilization Reports and Notes, and Technology Surveys.

Details on the availability of these publications may be obtained from:

SCIENTIFIC AND TECHNICAL INFORMATION DIVISION

NATIONAL AERONAUTICS AND SPACE ADMINISTRATION

Washington, D.C. 20546